



## A Review of the Effects of Key Parameters on the Performance of Horizontal and Vertical Axis Wind Turbines

Mohammed Atella Kamal<sup>1,2\*</sup>, Hussein Hayder Mohammed Ali<sup>1,2</sup>

<sup>1</sup> Department of Mechanical Power Techniques Engineering, Technical College Engineering Kirkuk, Northern Technical University, Kirkuk 36001, Iraq

<sup>2</sup> Renewable Energy Research Center Kirkuk, Northern Technical University, Kirkuk 36001, Iraq

Corresponding Author Email: [mohammed.atella23@ntu.edu.iq](mailto:mohammed.atella23@ntu.edu.iq)

Copyright: ©2025 The authors. This article is published by IIETA and is licensed under the CC BY 4.0 license (<http://creativecommons.org/licenses/by/4.0/>).

<https://doi.org/10.18280/jesa.580713>

### ABSTRACT

**Received:** 3 June 2025

**Revised:** 5 July 2025

**Accepted:** 14 July 2025

**Available online:** 31 July 2025

#### **Keywords:**

*renewable energy, vertical axis wind turbine (VAWT), horizontal axis wind turbine (HAWT), urban wind power, turbulent wind conditions*

Wind energy has emerged as one of the fastest-growing renewable energy sources, with horizontal axis wind turbines (HAWTs) predominantly deployed in large-scale applications. However, their effectiveness in urban environments is limited due to fluctuating wind patterns and space constraints. In contrast, vertical axis wind turbines (VAWTs) offer advantages such as compact design, low noise levels, and stable performance under low-speed and turbulent wind conditions, making them more suitable for urban settings. This review examines the performance characteristics of key VAWT configurations, including lift-based Darrieus turbines, drag-based Savonius turbines, and hybrid designs. Typical power coefficients ( $C_p$ ) for these designs are approximately 0.4 for Darrieus, 0.15-0.2 for Savonius, and 0.3-0.35 for hybrid models. Optimal operation is generally achieved at a tip speed ratio (TSR) of 0.45, corresponding to a maximum  $C_p$  of around 0.306 and a torque coefficient of 0.68. The review also identifies critical design and operational parameters influencing turbine performance. Finally, it highlights the need for continued research to enhance efficiency, reliability, and integration of VAWTs into future urban energy systems.

## 1. INTRODUCTION

In recent years, wind energy has become the most cost-effective renewable energy source, outperforming many conventional options in regions with favorable wind conditions. Modern wind turbine generators, built on well-established technologies, provide reliable and long-term power generation. Despite its competitiveness, wind power must continue evolving to remain viable amid emerging energy technologies and variable environmental conditions, especially in low wind speed scenarios where performance is limited.

Renewable energy sources, including solar, hydro, wind, and ocean energy, offer sustainable alternatives to fossil fuels. As concerns over pollution and fluctuating oil prices grow, the value of these clean energy options increases [1, 2]. Wind power, one of the fastest-growing renewable sectors, provides significant environmental benefits alongside energy generation.

Among wind turbine types, VAWTs such as Darrieus and Savonius designs are well-suited for urban settings. The Darrieus turbine, known for its high efficiency and ability to achieve tip speed ratios greater than one, suffers from self-starting limitations. In contrast, the Savonius rotor offers high torque at low wind speeds but with lower efficiency. Hybrid configurations combining H-Darrieus and Savonius rotors have shown promise in enhancing overall performance,

particularly for rooftop applications where wind direction is non-uniform. The aerodynamic acceleration effect caused by rooftop structures may further boost turbine output in urban environments [3-5].

## 2. WIND TURBINE

### 2.1 Horizontal axis wind turbine (HAWT)

The HAWTs has a rotor axis that is parallel to both the ground and the direction of the wind flow. Modern HAWTs typically use two or three blades. The primary role of the rotor is to convert the kinetic energy of the wind into rotational energy, which can then be utilized by a generator. The airfoil shape of the blades creates aerodynamic lift due to the pressure difference formed as wind accelerates on one side and slows on the other. This lift causes the blades to rotate around the hub in a plane perpendicular to it, while a drag force, acting perpendicular to the lift, resists this motion. The goal in wind turbine design is to achieve a high lift-to-drag ratio, which is optimized along the blade's length to maximize energy production at varying wind speeds. HAWTs offer several advantages, such as high efficiency compared to VAWTs, the ability to start independently without external power, and effective operation in high wind conditions. Additionally, they can adjust the angle of attack for optimal performance in low-

wind environments and harness wind energy efficiently due to the coordinated movement of all blades. However, HAWTs also have drawbacks, including the need for a large installation area, high setup and maintenance costs, inability to function at wind speeds below 5 m/s, sensitivity to wind direction, transportation challenges due to large components, noise pollution, and the necessity of being located far from urban areas. Irshad et al. [6] conducted a techno-economic analysis comparing hybrid renewable energy systems (HRES) using HAWT and VAWT axis wind turbines combined with solar PV and grid power. Using a Multi-Objective Genetic Algorithm in MATLAB, they found that HAWT-based systems are more cost-effective and efficient, with a lower cost of energy (\$0.02/kWh) and higher CO<sub>2</sub> emission savings (80.5%) compared to VAWT-based systems. The study highlights HAWT as the better option for rural electrification in terms of performance and sustainability. Zidane et al. [1] evaluated the impact of upstream deflectors on H-Darrieus VAWT performance using CFD simulations. Their results showed that deflectors significantly improve aerodynamic performance, increasing the maximum moment coefficient by up to 24% and enhancing average torque across various tip speed ratios. Chen et al. [7] review the performance and potential of VAWTs arranged in clusters. While individual VAWTs typically underperform compared to HAWTs, they exhibit higher power density in clusters due to positive wake interactions. The study explores aerodynamic behavior, structural dynamics, modeling, and optimization of VAWT clusters, highlighting their potential for improving wind farm efficiency and reducing energy costs. The paper also identifies research gaps and discusses future directions, including advanced control strategies and machine learning applications. van der Deijl et al. [8] conducted a wind tunnel study comparing the wake behavior of scaled HAWT and VAWT under low and moderate turbulence conditions. Using hot-wire anemometry, the study found that under low turbulence, VAWTs exhibit faster wake recovery than HAWTs. However, under moderate turbulence, the wake characteristics of both turbine types converge, showing similar velocity deficits and recovery behavior. The results highlight the influence of ambient turbulence on turbine wake dynamics and its implications for wind farm layout and performance.

Mokarram and Pham [9] used deep learning models and GIS tools to forecast energy production from HAWTs and VAWTs. They applied LSTM, LSTM-Wavelet, SVR, and Markov/CA-Markov models to analyze spatial and temporal energy output trends from 2000 to projected values in 2030. The LSTM-Wavelet hybrid model achieved the highest accuracy (over 90%) due to its ability to handle unstable data and reduce noise. Results showed a notable increase in wind energy potential, especially in northern regions, supporting improved wind energy planning and resource management.

Amroune et al. [10] focus on the balancing operation of turbine rotors, aiming to improve the distribution of rotor masses so that the free centrifugal forces around the rotor axis do not exceed the tolerances specified by the manufacturer. They propose algorithms that use data from an electronic scale measuring the static moment of turbine blades to determine the correction weight and the angular position of the correction mass. Additionally, they present a simulation of blade distribution to provide insights during assembly. This balancing process is essential during rotor repairs or the assembly of new flexible rotors, and the proposed methods are implemented using MATLAB.

Alam and Iqbal [11] present the design and development of a hybrid vertical axis turbine capable of extracting energy from wind or water currents regardless of flow direction. The proposed turbine combines a straight-bladed Darrieus (lift-type) rotor with a double-step Savonius (drag-type) rotor on a single shaft. This hybrid configuration leverages the self-starting ability of the Savonius turbine and the higher efficiency of the Darrieus turbine at elevated flow speeds. The system was constructed and tested in variable-speed water currents, demonstrating improved self-starting characteristics and enhanced power conversion performance. Additionally, the design is adaptable for use as a wind turbine and is intended for power generation applications on the sea floor for instrumentation systems.

Adnan et al. [12] investigate the enhancement of wind turbine performance by developing an optimal hybrid type-3 fuzzy logic controller (HT3-FPIDC) for blade pitch angle (BPA) control in horizontal axis wind turbines. Recognizing the limitations of type-1 and type-2 fuzzy controllers in handling high levels of uncertainty, the study introduces the type-3 fuzzy controller, which employs three-dimensional membership functions for improved decision-making. Six controller types, including type-1, type-2, type-3, and their respective hybrid fuzzy-PID configurations, are compared using Mamdani and Sugeno fuzzy inference systems. Genetic Algorithm (GA) and Particle Swarm Optimization (PSO) are used for tuning. Results from simulations on a 500 kW wind turbine indicate that the proposed HT3-FPIDC with Mamdani FIS and PSO yields the most stable and efficient power output, outperforming other controllers in terms of reduced absolute summation error and consistent rated power generation.

Alqurashi and Mohamed [13] analyze the aerodynamic forces acting on the blades of H-rotor Darrieus vertical axis wind turbines, particularly in low wind speed environments. The study evaluates three blade profiles, NACA 0021, LS413, and S1046 using CFD simulations to assess performance during rotation and static conditions. The results reveal that the symmetric S1046 airfoil generates higher aerodynamic forces in both dynamic and stationary states, while the NACA 0021 airfoil offers superior self-starting capability due to its lower aerodynamic torsion. The findings contribute to optimizing Darrieus rotor blade design for enhanced performance in remote or low-power applications. Tang et al. [14] conducted a laboratory investigation to evaluate the feasibility of using acoustic emission (AE) techniques for in-service structural health monitoring of wind turbine blades. A 45.7-meter blade, designed for a 2 MW generator, was subjected to simulated in-service cyclic loading over 21 days. An artificial defect was introduced to assess the system's sensitivity. AE monitoring successfully detected the growth of fatigue-related damage, including delamination and channel cracking. Signal triangulation using a four-sensor array enabled accurate damage localization. Chen et al. [15] propose an improved theoretical framework for estimating aerodynamic damping in HAWTs, addressing limitations of existing models that assume rigid blades and minimal shaft tilt or yaw. The new theory incorporates more realistic conditions, such as blade flexibility, shaft tilt, and yaw angles, to better capture aero-structural interactions. Comparisons with numerical results confirm the enhanced accuracy of the model. The study introduces modification factors to adjust the original theory and includes aerodynamic tower damping in a decoupled fatigue analysis framework, demonstrating its practical application in turbine design and analysis.

Ghorani et al. [16] numerically investigated the optimization of the Invelox wind delivery system integrated with a HAWT using a surrogate-based multi-objective approach. Using 3D CFD simulations and the Multi-Objective Particle Swarm Optimization (MOPSO) algorithm, the study enhanced Invelox's geometry, leading to a 64.7% increase in air mass flow and a 279.9% increase in wind power at the throat. However, when a HAWT was placed inside the optimal throat section, a significant pressure drop was observed, negatively impacting the system's overall efficiency, Figure 1 illustrates the HAWT.

Thangavelu et al. [17] investigated the aeroelastic performance of HAWTs with swept blades under various yaw angles using CFD and FEA simulations. The study compared swept and unswept blades at yaw angles of 0°, 10°, 30°, and 60° with a wind speed of 10 m/s. Results indicated that yaw misalignment negatively affects both blade types, but swept blades exhibited superior aeroelastic performance by achieving higher power output and experiencing lower structural deformation, thereby offering greater stability under yaw conditions. Krishnan et al. [18] focused on redesigning a HAWT blade to enhance its structural efficiency and reduce weight. Using a custom load generation code (V BLADE) and finite element analysis (FEA), the team optimized a composite blade with spar-rib construction. The redesign achieved a 39% reduction in blade weight while meeting static and buckling performance criteria, ultimately contributing to improved turbine efficiency and performance.

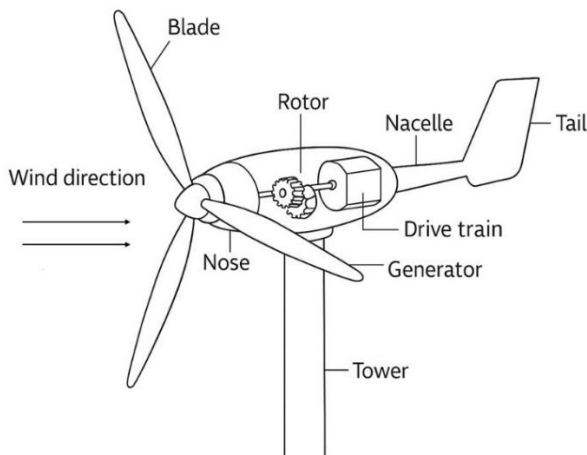


**Figure 1.** Horizontal axis wind turbine

Despite their efficiency, HAWTs face limitations in urban or low-wind environments due to their size, noise, and alignment requirements. As such, attention is shifting toward VAWTs for decentralized or small-scale applications where environmental adaptability is critical.

## 2.2 Vertical axis wind turbine (VAWT)

In VAWTs, the rotor's axis of rotation is perpendicular to both the wind direction and the ground. One key benefit of VAWTs is their ability to operate effectively even at low wind speeds. Among their notable advantages is the ability to function without directional adjustment, allowing them to harness wind from any direction an essential feature in locations with unpredictable wind patterns or obstructions. Maintenance is also more convenient and cost-effective due to the accessibility of components near the ground. Additionally,

VAWTs have a simple design that makes them easy to transport, install, and manufacture, resulting in lower initial investment costs compared to HAWTs. They are suitable for installation in residential areas, including rooftops or hilltops, and require less space than HAWTs, making them ideal for domestic use. However, VAWTs also have several disadvantages. Their efficiency typically ranges between 30–35%, which is lower than that of HAWTs. They are also more prone to vibration issues due to the turbulent airflow near the ground. Furthermore, support wires may be required to stabilize the structure. The two most common types of vertical axis wind turbines are the Darrieus and Savonius models. Ali et al. [19] conducted a 3D numerical study to assess the aerodynamic performance of a hybrid wind turbine configuration by integrating VAWTs around a HAWT tower. The research aimed to optimize VAWT positioning (0°, 45°, 60°, and 90° around the tower) to enhance power output. Findings showed that tower-induced flow acceleration improved VAWT performance at certain positions, especially 60° and 90°, where power coefficients reached 0.4864 and 0.5487, respectively. The hybrid setup also marginally increased the power output of the central HAWT by 0.83% when VAWTs were positioned at 90°. Rusli et al. [20] introduced a novel omni-directional flow concentrator (ODFC) to enhance the performance of cross-axis wind turbines (CAWTs), particularly in turbulent and low-speed wind environments such as urban or complex terrains. Unlike traditional flat plate deflectors, the ODFC improves vertical wind redirection and supports omni-directional operation. The design was optimized through CFD simulations by adjusting parameters like layer number, diameter, deflection angle, and fin count. The optimized system achieved vertical wind redirection of up to 76.33% of the initial speed, outperforming flat plate deflectors by 50.66%. Performance comparisons revealed enhancements of 100%, 150%, and 12% over CAWT-flat plate, VAWT, and HAWT configurations, respectively. A scaled-up version of the CAWT-ODFC achieved a power coefficient of 0.50, demonstrating its potential for efficient energy capture in diverse and challenging wind conditions, as the details are shown in Figure 2. Wenehenubun et al. [21] investigate the impact of blade number on the performance of Savonius-type VAWTs. Through experimental testing of turbines with 2, 3, and 4 blades, the study evaluates performance metrics including tip speed ratio, torque, and power coefficient under varying wind speeds. Complementary simulations using ANSYS 13.0 illustrate the pressure distribution on turbine blades. The findings reveal that blade count significantly influences turbine efficiency, with the three-bladed configuration demonstrating optimal performance at higher tip speed ratios, reaching a maximum of 0.555 at 7 m/s wind speed. The fundamental design equations for both HAWTs and VAWTs can be written as:

$$P = C_p \cdot \frac{1}{2} \rho A V^3 \quad (1)$$

$$\sigma = N_c / \pi R \quad (2)$$

Blade Element Momentum Theory (BEMT) for wind turbine can be found from the following equation:

$$dT = \frac{1}{2} \rho \omega^2 c C_L \cos(\phi) \quad (3)$$

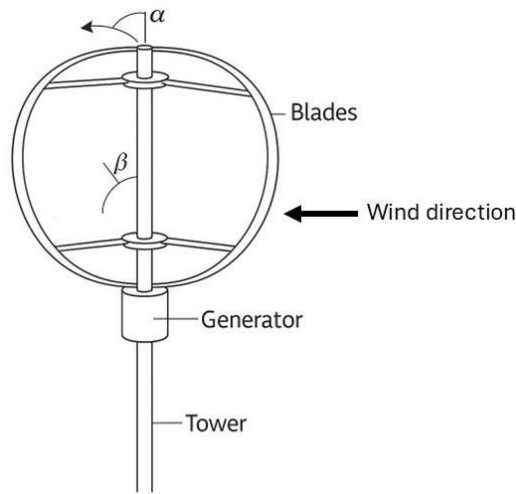


**Figure 2.** Vertical axis wind turbine

These studies collectively suggest that VAWTs, although less efficient than HAWTs in terms of  $C_p$ , offer significant advantages in installation flexibility, maintenance, and performance under variable wind conditions, making them promising for small-scale and urban deployment.

### 2.2.1 Darrieus rotor

A Darrieus rotor is formed by positioning a vertical airfoil at a certain distance or angle from an axis that runs vertically. These wind turbines harness the wind's kinetic energy by letting the airfoil travel at the speed of the wind. They spin at a high rate and have a lot of power, but they can't launch themselves very well [8].

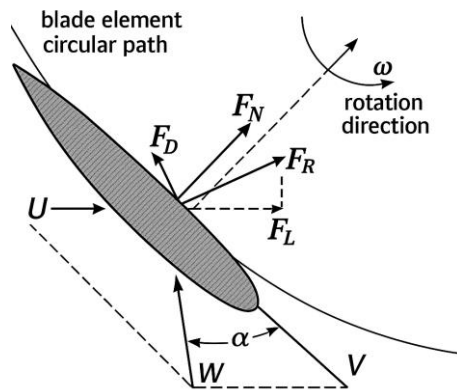


**Figure 3.** Darrieus blade speed and power direction diagram

Two or more airfoil turbine blades are positioned on a vertical rod that moves within a Darrieus turbine. The wind's action on the airfoil turbine blades results in lift, this propulsive force causes the turbine blades to move forward. Various aerodynamic effects caused by the passage of air through the turbine's rotor may have an effect on the shape of the turbine's blades. The two most important terms associated with these forces are air drag ( $F_D$ ) that acts in the direction of the flow and lift ( $F_L$ ) that acts perpendicular to the flow. These forces are associated with the wind's angle of attack  $\alpha$  in a close manner. The relative velocity  $W$  has an effect on the local angle of attack ( $\alpha$ ), which is altered by the rotation of the rotor blades.  $W$  is determined by the combination of two variables: the local velocity induced by the rotor ( $U$ ) and the rotational speed of the blades ( $V$ ). As demonstrated in Figure

3, the torque and power are derived from the tangential force  $F_T$  and the normal force  $F_N$ . Many varieties of Darrieus generators exist, including H-rotors, eggbeaters, spunky blades, and twists.

### 2.2.2 Savonius VAWT

The Savonius turbine is a vertical-axis wind turbine that uses drag to generate power. Designed by Finnish scientist Sigurd Johannes Savonius, it typically has two to four semi-cylindrical rotor blades arranged vertically. A two-blade design forms an "S" shape in cross-section (Figure 4). The concave blades face the wind and drive the rotation, while the convex blades oppose the wind with less resistance. This difference in resistance creates torque, causing the turbine to spin. Though simple and robust, the Savonius turbine is less efficient than other designs. Figure 5 show variations in blade orientation and design types.

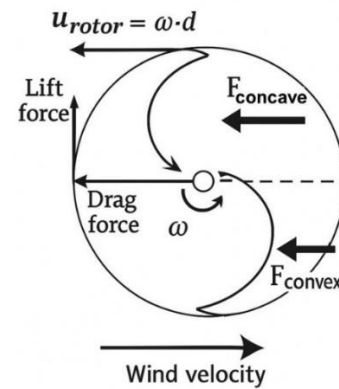


**Figure 4.** Schematic diagram illustrating the drag forces acting on two different Savonius blades

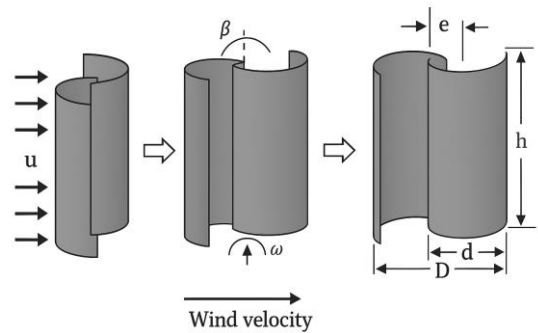


**Figure 5.** Schematic diagram of a two-bladed Savonius rotor shown at various angular positions in the clockwise direction

Key performance parameters commonly used in wind turbine analysis include the tip speed ratio ( $\lambda$ ), torque coefficient ( $C_t$ ), and moment coefficient ( $C_m$ ). The tip speed ratio denoted as  $\lambda$ , is defined as the ratio of the blade tip speed to the incoming wind speed and is expressed as  $\lambda = \frac{\omega R}{V}$ , where  $\omega$  is the angular velocity,  $R$  is the rotor radius, and  $V$  is the wind speed. It plays a crucial role in determining turbine efficiency, with higher TSR values typically associated with lift-based turbines like Darrieus, while drag-based turbines like Savonius operate best at lower  $\lambda$ s. The  $C_T$  is a dimensionless parameter that quantifies the torque generated by the turbine relative to the dynamic pressure of the wind and is calculated using the equation  $C_t = \frac{T}{0.5 \rho A R V^2}$ , where  $T$  is torque,

$\rho$  is air density, and  $A$  is the swept area. This coefficient is vital for evaluating the turbine's ability to generate torque under varying wind conditions. Similarly, the moment coefficient ( $C_m$ ) represents the non-dimensional form of the aerodynamic moment acting on the rotor and is given by  $C_m = \frac{M}{0.5\rho A R V^2}$ , where  $M$  is the aerodynamic moment. In some literature,  $C_T$  and  $C_m$  are used interchangeably, although  $C_m$  may sometimes refer to localized blade moment coefficients in detailed aerodynamic studies. These parameters collectively aid in comparing and optimizing the aerodynamic and structural performance of different wind turbine configurations.

### 3. PERFORMANCE AND RELIABILITY OF VERTICAL AXIS WIND TURBINES

Many models have been developed by researchers and scientists to evaluate the efficiency of wind turbines. Here you can find a brief overview of the different models.

Dennis et al. [22] utilized CFD analysis to compare two twisted-blade VAWT designs and found improved pressure and torque characteristics for urban applications. Lin et al. [23] introduced a tubercle-modified trailing edge and demonstrated a 16.4% increase in power coefficient compared to straight blades. This result aligns with Sun et al. [24] further examined the influence of blade moment of inertia and shape by comparing the S-1046 and NACA0018 profiles. Their findings reinforce those of Lin et al. [23] and Castelli et al. [25] developed a CFD model to predict the aerodynamic performance of straight-bladed vertical-axis Darrieus wind turbines. By integrating principles from Blade Element-Momentum (BE-M) theory into the CFD framework, the study enabled detailed correlation between geometric parameters such as blade angle of attack and dynamic responses, including rotor torque and blade forces. The model was validated against experimental data and applied to simulate a classical NACA0021 three-bladed rotor across various tip speed ratios. The analysis provided insights into flow behavior under different operating conditions and revealed key trends in  $C_p$  variation. Finally, the effect of profile geometry on rotor performance. Three rotor blades, a wind speed of 9 m/s, a rotor height of 515 mm and a blade depth of 85.8 mm were the most important geometric parameters. The results show that the

overall aerodynamic performance of the DU06W200 is about 2% higher than that of the NACA0021, mainly due to the improved blade performance when running downwind. During the operation of VAWT blades, the azimuth position corresponds to the maximum torque value. In terms of predictive modeling, Sunny and Kumar [26] validated aerodynamic simulations in wind tunnels, which complemented Raciti Castelli's computational approach. However, while many studies report promising simulation results, relatively few validate these findings experimentally, highlighting a research gap in empirical verification and long-term reliability testing.

Battisti et al. [27], suggesting that thinner symmetric blades like S-1046 offer improved fatigue performance and self-starting behavior, especially under low wind speeds. Battisti et al. also explored the effect of blade pitch and airfoil asymmetry, concluding that asymmetric profiles (e.g., DU06W200) provide better performance at low tip speed ratios, supporting findings from Castelli et al. [25] and Douak et al. [28].

A notable point of convergence across these studies is the superior performance of hybrid configurations. For instance, Feng et al. [29] showed that combining Savonius and Darrieus geometries can offset the poor self-starting ability of straight-bladed Darrieus turbines, a problem also addressed by Douak et al. through optimal angle of attack control. Similarly, Kavade and Ghanegaonkar [30] compared various combinations of Savonius and Darrieus blades and identified the 3+3 blade hybrid as the most efficient at wind speeds between 2–8 m/s.

Finally, while various researchers have addressed individual performance aspects such as vortex control [23], fatigue [24], and torque optimization [29] there remains a need for integrated studies that simultaneously optimize aerodynamic, structural, and control parameters. Additionally, the impact of urban turbulence, rotor placement, and multi-rotor interactions is underexplored and represents an important avenue for future work. Compared to the other combinations, the HVAWT results show that the model with three Savonius blades and three Darrieus blades produces the best turbine performance in the wind speed range of 2-8 m/s. The CP of this model is 0.23, which is higher than the other combinations as well as the single Savonius and Darrieus turbines at low wind speeds. Details in Table 1 Summarizing the experimental and numerical results [31-39].

**Table 1.** Summary of key VAWT/Savonius turbine studies

Ref.	Turbine Type	Blade Shape / Design	No. of Blades	Key Parameters Studied	Peak Power or $C_p$	Methodology	Key Findings
[31]	Straight-bladed H-type VAWT	NACA 0021 (symmetrical)	2 to 5	Tangential & normal forces vs. azimuth angle	Power coefficient decreases with blade number	Wind tunnel + pressure sensors	Upstream region (0°–180°) most influential for power
[32]	H-type Darrieus VAWT	Straight airfoil blades	3	Solidity effect, TSR range	Not explicitly stated	CFD (Realizable k- $\epsilon$ )	TSR range & self-starting behavior depend on solidity 5.9% higher measured output than model prediction
[33]	Helical-blade VAWT	NACA 0018	Not specified	Power output vs. wind speed	114.7 W at 9 m/s	Wind tunnel + CFD	Aspect ratio (H/c) critical for torque/power
[34]	Savonius (SSWT)	Semicircular	2	Torque, Power vs. dimensions (via DE)	Reduced turbine area by 9.8%	Inverse optimization + experiment	Realizable k- $\epsilon$ most accurate; novel
[35]	Savonius	Classical, elliptical, novel	Various	Effect of blade shape & overlap	Highest $C_p$ for novel blade	2D CFD + experiment	

				ratio			blade best
[36]	Savonius	Varies	Varies	Parametric study over decades	Efficiency improvement trends	Review + computational studies	Proper CFD choice crucial for optimization
[37]	Savonius	Two-bladed novel design	2	Power and torque coefficients, Reynolds number effect, blockage correction	34.8% gain in maximum power coefficient	Wind tunnel experiments	Novel two-bladed turbine outperforms semicircular, semi-elliptic, Benesh and Bach blades
[38]	Savonius	Semicircular (varying overlap)	2	Static/dynamic torque vs. overlap ratio	Optimum Cp at 0.15 overlap	CFD with SST k- $\omega$	Overlap enhances returning blade torque
[39]	Two-stage Savonius (Hydrokinetic)	Semicircular	2 per stage $\times$ 2	TSR vs. flow speed & generator efficiency	Cp $\sim$ 0.43 at 0.26 m/s	Flume & sea tests	Generator upgrade increased efficiency from 15% to 43%

### 3.1 Numerical methods

To enhance aerodynamic performance, the cross-sectional geometry of HAWT blades is typically composed of two-dimensional (2D) airfoil profiles. These airfoils are generally arranged along a predefined coordinate system, with the local radial spacing between them determined by the number and distribution of the airfoils. Bai and Wang [40] proposed that the aerodynamic center of each airfoil section should be aligned with the origin of the coordinate system during the blade's construction process. The optimal chord length and pitch angle for each blade section can be systematically determined through the Blade Element Momentum (BEM) method. The final three-dimensional (3D) blade configuration, including the hub, can subsequently be developed using advanced Computer-Aided Design (CAD) tools. Two principal methodologies are commonly employed to simulate the rotational dynamics of HAWT blades. The first involves the Moving Reference Frame (MRF) technique, which approximates steady-state flow behavior across a rotating blade. Under this method, aerodynamic performance can be evaluated using a single blade model with periodic boundary conditions, thereby reducing computational cost. The second approach, known as the Sliding Mesh technique, is more suitable for resolving unsteady or transient flow phenomena. This method necessitates the use of a full-scale rotor model, which significantly increases computational demand due to the extensive mesh resolution required. Furthermore, it involves two domains in relative motion one of which is a cylindrical region surrounding the rotor resulting in non-conformal mesh interfaces due to the rotational motion. For the boundary conditions, inflow velocity and outflow pressure are typically prescribed at the inlet and outlet boundaries, respectively. A no-slip condition is enforced on all solid surfaces, including the turbine blades and hub. When employing the MRF approach, periodic boundary conditions are commonly applied to model a single blade segment effectively.

Mesh generation is typically carried out using specialized tools such as Gambit, Pointwise, or ICEM-CFD. To accurately capture the velocity profile within the blade's boundary layer, structured grids are often used to maintain a precise distance between the wall and the first adjacent grid node. The computational domain encompassing both upstream and downstream regions of the turbine is then discretized using either structured or unstructured meshes, depending on the complexity of the geometry. The non-dimensional wall distance, denoted as  $y^+$ , is calculated to evaluate the grid spacing near the wall, ensuring adequate resolution of boundary layer effects.

Predicting with any degree of accuracy when a flow will

separate from a smooth surface is one of the several issues with turbulence models. Under unfavorable pressure gradient conditions, the commencement and quantity of flow separation are often not predicted by the classic two-equation turbulence models. For this purpose, aerodynamic researchers have created a slew of sophisticated turbulence models. The previous studies used the 3D SST k- $\omega$  turbulence model, which agrees with the experimental work. Peng et al. [41] investigated the aeroelastic behavior and structural responses of flexible blades on HAWTs subjected to typhoon conditions. Using a coupled fluid-structure interaction approach combining CFD and finite element methods (FEM), they studied how aeroelasticity and wind direction relative to the rotor plane affect the aerodynamic forces and blade dynamics under low-turbulence typhoon winds. Their results showed that at a wind direction of  $90^\circ$  (perpendicular to the rotor plane), blade thrust fluctuations were significantly higher due to vortex shedding from the upstream blade, which amplified aerodynamic loading on downstream blades. This led to a 109.3% increase in flap wise thrust on a specific blade (Blade 3 at azimuth  $240^\circ$ ). However, aeroelastic effects also caused displacement-induced flow separation that increased aerodynamic damping, which in turn reduced blade-tip displacement and blade-root moment fluctuations, lowering the maximum blade stress. Overall, the vortex shedding at  $90^\circ$  wind direction improved the structural safety of HAWTs during typhoon events by modulating aerodynamic loads and blade responses. The transient forces acting on a wind turbine with a vertical axis can be studied using this model. Good results can only be achieved with a small value of  $Y^+$  ( $Y^+ \leq 1$ ). The  $Y^+$  does not  $Y^+$  is a measure of the relative magnitude of turbulent and laminar influences within a cell; a large value indicates turbulent behavior, whereas a small value indicates laminar behavior. Determining the appropriate size of the cells near domain barriers is crucial in turbulence modelling. One of the most reliable eddy-viscosity turbulence models used in CFD is the shear stress transfer (SST) model. The SST model is a combination of the k- $\omega$  and k- $\epsilon$  turbulence models; the former is applied to the inner boundary layer region, while the latter is utilized to transition to the free shear flow.

Amroune et al. [42] present a reverse engineering approach for the design and manufacturing of complex-shaped mechanical parts, particularly those lacking technical drawings or degraded by wear. The process begins with data acquisition using a 3D scanner or a measuring machine tool (MMT) to generate a point cloud, which is then processed in CAD software (CATIA) to create a detailed digital model. This model serves as the basis for producing a physical prototype using 3D printing (additive manufacturing). The printed part is subsequently used to form an imprint in sand

moulds through a fusion process. This method significantly reduces model preparation time and is easy to implement in industrial settings. Additionally, structural analysis using finite element (FE) tools was applied to assess product quality, showing that Von Mises equivalent stresses and strains decreased with increased surface area and honeycomb thickness. The study aims to demonstrate the practicality and

benefits of integrating reverse design with additive manufacturing and simulation in modern production workflows. Table 2 shows comparison between HAWTs and VAWTs focusing on key performance indicators like power coefficient ( $C_p$ ), tip speed ratio ( $\lambda$ ), and other relevant factors.

**Table 2.** Comparison of HAWTs and VAWTs on key performance indicators

Feature/Indicator	HAWT (Horizontal Axis Wind Turbine)	VAWT (Vertical Axis Wind Turbine)
Typical Power Coefficient ( $C_p$ )	0.35 – 0.45 (up to 0.5 in optimized designs)	0.2 – 0.35 (usually lower due to drag and dynamic stall)
Typical Tip Speed Ratio (TSR)	6 – 8 (high TSR for efficient energy capture)	1 – 4 (lower TSR due to design and starting torque)
Self-starting capability	Generally good, requires yaw control	Good in many designs (e.g., Savonius is self-starting)
Yaw mechanism	Required to align rotor to wind direction	Not required due to omnidirectional wind capture
Complexity & Maintenance	More complex (gearbox, yaw system)	Simpler mechanically, easier maintenance
Noise generation	Moderate to high	Generally quieter due to lower tip speeds
Suitability for urban environments	Limited due to size and noise	More suitable for urban and turbulent wind conditions
Start-up torque	Lower startup torque	Higher startup torque, especially Savonius types
Typical blade number	2 or 3 blades	2 to 5 blades common
Aerodynamic efficiency	Higher due to lift-driven design	Lower, influenced by drag and unsteady aerodynamics
Typical applications	Utility-scale wind farms	Small-scale and urban power generation

4. CONCLUSIONS

This review has systematically analyzed the key parameters affecting the performance of vertical axis wind turbines (VAWTs), with a focus on Darrieus (lift-based), Savonius (drag-based), and hybrid configurations. Among these, straight-bladed Darrieus turbines exhibit strong potential for efficient operation in low-wind conditions, while Savonius rotors are advantageous for their self-starting ability and torque generation. Hybrid designs, which integrate the benefits of both types, show promise for achieving enhanced performance and operational stability under fluctuating wind conditions.

Current research trends highlight the critical influence of design parameters such as airfoil geometry, blade number, aspect ratio, overlap ratio, and rotor solidity on performance indicators like the power coefficient ( $C_p$ ), torque coefficient ( $C_t$ ), and startup behavior. Optimization of the tip speed ratio ( $\lambda$ ) and consideration of Reynolds number effects remain central to performance enhancement across different scales. Notably, recent advancements in bio-inspired and asymmetric airfoil profiles have led to measurable improvements in aerodynamic efficiency, particularly in urban and low-speed environments.

Despite these developments, several technical challenges persist. These include performance variability in complex wind conditions, high production and maintenance costs, and limited integration into urban energy infrastructure. To address these issues, future research should prioritize the development of adaptive rotor designs, advanced computational models capable of capturing transient and turbulent flows, and robust control strategies for urban deployment. Moreover, expanding the scope of VAWT applications to include energy harvesting from industrial exhausts and other non-traditional sources could further enhance their utility.

REFERENCES

[1] Zidane, I.F., Ali, H.M., Swadener, G., Eldrainy, Y.A.,

Shehata, A.I. (2023). Effect of upstream deflector utilization on H-Darrieus wind turbine performance: An optimization study. *Alexandria Engineering Journal*, 63: 175-189. <https://doi.org/10.1016/j.aej.2022.07.052>

[2] Ali, H.H.M., Ahmed, S.Y. (2024). Assessing the economic viability of solar distillation employing a rotating hollow cylinder. *International Journal of Heat and Technology*, 42(2): 613-619. <https://doi.org/10.18280/ijht.420228>

[3] Amroune, S., Mohamad, B., Moussaoui, M., Saaidi, H. (2018). Geometric regeneration and mechanical analysis of a gas turbine blade type Frame 9001 GE. *Engineering Solid Mechanics*, 6(2): 105-112. <https://doi.org/10.5267/j.esm.2018.3.003>

[4] Hussein, A.M., Ali, H.H.M., Ali, Z. (2024). Assessing the efficacy of flat-plate solar collectors using nanofluids in the climatic context of Kirkuk city, Iraq. *Acta Polytechnica*, 64(1): 25-33. <https://doi.org/10.14311/AP.2024.64.0025>

[5] Mertens, S., van Kuik, G., van Bussel, G. (2003). Performance of an H-Darrieus in the skewed flow on a roof. *Journal of Solar Energy Engineering*, 125(4): 433-440. <https://doi.org/10.1115/1.1623392>

[6] Irshad, A.S., Kargar, N., Elkholy, M.H., Ludin, G.A., et al. (2024). Techno-economic evaluation and comparison of the optimal PV/Wind and grid hybrid system with horizontal and vertical axis wind turbines. *Energy Conversion and Management*: X, 23: 100638. <https://doi.org/10.1016/j.ecmx.2024.100638>

[7] Chen, C., Ageze, M.B., Tigabu, M.T. (2024). Perspectives of vertical axis wind turbines in cluster configurations. *Fluid Dynamics & Materials Processing*, 20(12): 613-619. <https://doi.org/10.32604/fdmp.2024.058169>

[8] van der Deijl, W., Schmitt, F., Sicot, C., Barre, S., Hölling, M., Obligado, M. (2024). Effect of background turbulence on the wakes of horizontal-axis and vertical-axis wind turbines. *Journal of Wind Engineering and Industrial Aerodynamics*, 253: 105877. <https://doi.org/10.1016/j.jweia.2024.105877>

[9] Mokarram, M., Pham, T.M. (2024). Predicting wind turbine energy production with deep learning methods in

- GIS: A study on HAWTs and VAWTs. *Sustainable Energy Technologies and Assessments*, 72: 104070. <https://doi.org/10.1016/j.seta.2024.104070>
- [10] Amroune, S., Belaadi, A., Menasri, N., Zaoui, M., Mohamad, B., Amin, H. (2019). New approach for computer-aided static balancing of turbines rotors. *Diagnostyka*, 20(4): 95-101. <https://doi.org/10.29354/diag/114621>
- [11] Alam, M.J., Iqbal, M.T. (2009). Design and development of hybrid vertical axis turbine. In 2009 Canadian Conference on Electrical and Computer Engineering, pp. 1178-1183. <https://doi.org/10.1109/CCECE.2009.5090311>
- [12] Adnan, A.Q., Hussain, M.K., Mohammadzadeh, A., Sabahi, K. (2025). Optimal hybrid type-3 fuzzy controller for horizontal axis wind turbines: Comparative study. *ISA Transactions*. <https://doi.org/10.1016/j.isatra.2025.03.025>
- [13] Alqurashi, F., Mohamed, M.H. (2020). Aerodynamic forces affecting the h-rotor darrieus wind turbine. *Modelling and Simulation in Engineering*, 2020(1): 1368369. <https://doi.org/10.1155/2020/1368369>
- [14] Tang, J., Soua, S., Mares, C., Gan, T.H. (2016). An experimental study of acoustic emission methodology for in service condition monitoring of wind turbine blades. *Renewable Energy*, 99: 170-179. <https://doi.org/10.1016/j.renene.2016.06.048>
- [15] Chen, Y., Wu, D., Yu, Y., Gao, W. (2021). An improved theory in the determination of aerodynamic damping for a horizontal axis wind turbine (HAWT). *Journal of Wind Engineering and Industrial Aerodynamics*, 213: 104619. <https://doi.org/10.1016/j.jweia.2021.104619>
- [16] Ghorani, M.M., Karimi, B., Mirghavami, S.M., Saboohi, Z. (2023). A numerical study on the feasibility of electricity production using an optimized wind delivery system (Invelox) integrated with a horizontal axis wind turbine (HAWT). *Energy*, 268: 126643. <https://doi.org/10.1016/j.energy.2023.126643>
- [17] Thangavelu, S.K., Chow, S.F., Sia, C.C.V., Chong, K.H. (2021). Aeroelastic performance analysis of horizontal axis wind turbine (HAWT) swept blades. *Materials Today: Proceedings*, 47: 4965-4972. <https://doi.org/10.1016/j.matpr.2021.04.315>
- [18] Krishnan, B.P., Mathanbabu, M., Sathyamoorthy, G., Gokulnath, K., Kumar, L.G.S. (2021). Performance estimation and redesign of horizontal axis wind turbine (HAWT) blade. *Materials Today: Proceedings*, 46: 8025-8031. <https://doi.org/10.1016/j.matpr.2021.02.777>
- [19] Ali, K., Zhao, Z., Liu, Y., Liu, Y., et al. (2025). Numerical investigation of the position effect on a hybrid wind turbine model: Integrating vertical axis wind turbines around a horizontal axis wind turbine tower. *Sustainable Energy Technologies and Assessments*, 76: 104304. <https://doi.org/10.1016/j.seta.2025.104304>
- [20] Rusli, C.C., Kong, K.K., Khoo, S.Y., Long, S.X., Chong, W.T. (2025). Performance enhancement of cross-axis-wind-turbine: Design and CFD analysis of an omnidirectional flow concentrator. *Alexandria Engineering Journal*, 127: 500-521. <https://doi.org/10.1016/j.aej.2025.05.034>
- [21] Wenenubun, F., Saputra, A., Sutanto, H. (2015). An experimental study on the performance of Savonius wind turbines related with the number of blades. *Energy Procedia*, 68: 297-304. <https://doi.org/10.1016/j.egypro.2015.03.259>
- [22] Dennis, D., Ganesh, P.S., Joy, J., Amjith, L.R., Bavanish, B. (2022). Computational design & analysis of vertical axis wind turbine. *Materials Today: Proceedings*, 66: 1501-1508. <https://doi.org/10.1016/j.matpr.2022.06.407>
- [23] Lin, S.Y., Lin, Y.Y., Bai, C.J., Wang, W.C. (2016). Performance analysis of vertical-axis-wind-turbine blade with modified trailing edge through computational fluid dynamics. *Renewable Energy*, 99: 654-662. <https://doi.org/10.1016/j.renene.2016.07.050>
- [24] Sun, X., Zhu, J., Hanif, A., Li, Z., Sun, G. (2020). Effects of blade shape and its corresponding moment of inertia on self-starting and power extraction performance of the novel bowl-shaped floating straight-bladed vertical axis wind turbine. *Sustainable Energy Technologies and Assessments*, 38: 100648. <https://doi.org/10.1016/j.seta.2020.100648>
- [25] Castelli, M.R., Englaro, A., Benini, E. (2011). The Darrieus wind turbine: Proposal for a new performance prediction model based on CFD. *Energy*, 36(8): 4919-4934. <https://doi.org/10.1016/j.energy.2011.05.036>
- [26] Sunny, K.A., Kumar, N.M. (2016). Vertical axis wind turbine: Aerodynamic modelling and its testing in wind tunnel. *Procedia Computer Science*, 93: 1017-1023. <https://doi.org/10.1016/j.procs.2016.07.305>
- [27] Battisti, L., Brighenti, A., Benini, E., Castelli, M.R. (2016). Analysis of different blade architectures on small VAWT performance. *Journal of Physics: Conference Series*, 753(6): 062009. <https://doi.org/10.1088/1742-6596/753/6/062009>
- [28] Douak, M., Aouachria, Z., Rabehi, R., Allam, N. (2018). Wind energy systems: Analysis of the self-starting physics of vertical axis wind turbine. *Renewable and Sustainable Energy Reviews*, 81: 1602-1610. <https://doi.org/10.1016/j.rser.2017.05.238>
- [29] Feng, F., Li, S., Li, Y., Xu, D. (2012). Torque characteristics simulation on small scale combined type vertical axis wind turbine. *Physics Procedia*, 24: 781-786. <https://doi.org/10.1016/j.phpro.2012.02.116>
- [30] Kavade, R.K., Ghanegaonkar, P.M. (2017). Design and analysis of vertical axis wind turbine for household application. *Journal of Clean Energy Technologies*, 5(5): 353-358. <https://doi.org/10.18178/JOCET.2017.5.5.397>
- [31] Li, Q.A., Maeda, T., Kamada, Y., Murata, J., Furukawa, K., Yamamoto, M. (2015). Effect of number of blades on aerodynamic forces on a straight-bladed Vertical Axis Wind Turbine. *Energy*, 90: 784-795. <https://doi.org/10.1016/j.energy.2015.07.115>
- [32] Parra-Santos, M.T., Uzarraga, C., Gallegos, A., Castro, F. (2015). Influence of solidity on vertical axis wind turbines. *International Journal of Applied Mathematics Electronics and Computers*, 3(3): 215-217. <https://doi.org/10.18100/ijamec.42848>
- [33] Han, D., Heo, Y.G., Choi, N.J., Nam, S.H., Choi, K.H., Kim, K.C. (2018). Design, fabrication, and performance test of a 100-W helical-blade vertical-axis wind turbine at low tip-speed ratio. *Energies*, 11(6): 1517. <https://doi.org/10.3390/en11061517>
- [34] Roy, S., Das, R., Saha, U.K. (2018). An inverse method for optimization of geometric parameters of a Savonius-style wind turbine. *Energy Conversion and Management*, 155: 116-127. <https://doi.org/10.1016/j.enconman.2017.10.088>
- [35] Saeed, H.A.H., Elmekawy, A.M.N., Kassab, S.Z. (2019).



- Numerical study of improving Savonius turbine power coefficient by various blade shapes. Alexandria Engineering Journal, 58(2): 429-441. <https://doi.org/10.1016/j.aej.2019.03.005>
- [36] Roy, S., Saha, U.K. (2013). Review on the numerical investigations into the design and development of Savonius wind rotors. Renewable and Sustainable Energy Reviews, 24: 73-83. <https://doi.org/10.1016/j.rser.2013.03.060>
- [37] Roy, S., Saha, U.K. (2015). Wind tunnel experiments of a newly developed two-bladed Savonius-style wind turbine. Applied Energy, 137: 117-125. <https://doi.org/10.1016/j.apenergy.2014.10.022>
- [38] Nasef, M.H., El-Askary, W.A., Abdel-Hamid, A.A., Gad, H.E. (2013). Evaluation of Savonius rotor performance: Static and dynamic studies. Journal of Wind Engineering and Industrial Aerodynamics, 123: 1-11. <https://doi.org/10.1016/j.jweia.2013.09.009>
- [39] Tu, Q., Ji, S., Li, X., Zhang, X., Wu, S., Liu, H. (2025). Performance evaluation of a pilot-scale two-stage Savonius turbine for low-speed flow. Ocean Engineering, 330: 121288. <https://doi.org/10.1016/j.oceaneng.2025.121288>
- [40] Bai, C.J., Wang, W.C. (2016). Review of computational and experimental approaches to analysis of aerodynamic performance in horizontal-axis wind turbines (HAWTs). Renewable and Sustainable Energy Reviews, 63: 506-519. <https://doi.org/10.1016/j.rser.2016.05.078>
- [41] Peng, H.Y., Lin, Q.B., Liu, H.J. (2025). Effects of aeroelasticity and wind direction on the aerodynamic characteristics and structural responses of blades for horizontal-axis wind turbines under typhoons. Journal of Wind Engineering and Industrial Aerodynamics, 263: 106125. <https://doi.org/10.1016/j.jweia.2025.106125>
- [42] Amroune, S., Belaadi, A., Zaoui, M., Menaseri, N., Mohamad, B., Saada, K., Benyettou, R. (2021). Manufacturing of rapid prototypes of mechanical parts using reverse engineering and 3D Printing. Journal of the Serbian Society for Computational Mechanics, 15(1): 167-176. <https://doi.org/10.24874/jsscm.2021.15.01.11>

## NOMENCLATURE

Y+	boundary layers
CFD	computational fluids mechanic
g	gravitational acceleration, m.s <sup>-2</sup>
k	thermal conductivity, W.m <sup>-1</sup> . K <sup>-1</sup>
Nu	local Nusselt number along the heat source
Ex <sub>f</sub>	wind flow energy
Ex <sub>k</sub>	kinematic energy
Ex <sub>p</sub>	physical energy
TI	approach-flow total turbulence intensity [%]
SST	shear stress transfer
FL	lift force
FD	drag force
FN	normal force
FT	tangential force
dT	thrust on an element

## Greek symbols

ψ	exergy energy
λ	tip speed ratio
η	efficiency
σ	aolidity
α	angle of attack
β	rotor blade angle
Ω	rotational speed
ω	angular velocity
θ	azimuth angle
e	overlap distance

## Subscripts

A	swept area for (Savonius, Darrieus)
c	blade chord
C <sub>p</sub>	power coefficient
CT	torque coefficient
C <sub>md</sub>	dynamic torque coefficient
V <sub>∞</sub>	free stream velocity
D	rotor diameter
d	Savonius blade chord
h	height of the blade (Savonius)
H	height of the blade (Darrieus)
K	correction factor
u	wind velocity
U	wind velocity
N	number of blade
CL	lift coefficient
φ	inflow coefficient